Growing Polymer Brushes from a Variety of Substrates under Ambient Conditions by Cu^0-Mediated Surface-Initiated ATRP

Wenqing Yan,[1] Marco Fantin,[2] Shivaprakash Ramakrishna,[1]

Nicholas D. Spencer,[1] Krzysztof Matyjaszewski,[2]* Edmondo M. Benetti[1,3]**

[1]Laboratory of Surface Science and Technology, Department of Materials, Swiss Federal Institute of Technology (ETH Zürich), Vladimir-Prelog-Weg 1-5/10, CH-8093 Zurich, Switzerland

[2]Department of Chemistry, Carnegie Mellon University, 4400 Fifth Avenue, Pittsburgh, PA 15213, USA

[3]Swiss Federal Laboratories for Materials Science and Technology (Empa), Lerchenfeldstrasse 5, CH-9014, St. Gallen, Switzerland

This document is the accepted manuscript version of the following article:

Yan, W., Fantin, M., Ramakrishna, S. N., Spencer, N., Matyjaszewski, K., & Benetti, E. M. (2019). Growing polymer brushes from a variety of substrates under ambient conditions by CuO-mediated surface-initiated ATRP. ACS Applied Materials and Interfaces. https://doi.org/10.1021/acsami.9b09529

Keywords: polymer brushes; controlled radical polymerization; thin films; lubrication; atomic force microscopy

Abstract

Cu^0-mediated surface-initiated ATRP is a highly versatile, oxygen-tolerant, and extremely controlled polymer-grafting technique that enables the modification of flat inorganic surfaces, as well as porous organic and polymeric supports of different compositions. Exploiting the intimate contact between a copper plate, acting as source of catalyst and reducing agent, and an initiator-bearing support, Cu^0 SI-ATRP enables the rapid growth of biopassive, lubricious brushes from large flat surfaces, as well as from various organic supports, including cellulose fibres and elastomers, by using microliter volumes of reaction mixtures, and without the need for deoxygenation of reaction mixtures or an inert atmosphere. Thanks to a detailed analysis of its mechanism and the parameters governing the polymerization process, polymer brush-growth by Cu^0 SI-ATRP can be precisely modulated and adapted to be applied to morphologically and chemically different substrates, setting up the basis for translating SI-ATRP methods from academic studies into technologically relevant surface-modification approaches.

INTRODUCTION

The synthesis of polymer brushes by surface-initiated reversible-deactivation radical polymerization (SI-RDRP), and their subsequent application in a variety of materials formulations have been the subjects of a significant number of academic studies over the last two decades.[1-4] Although "grafted-from" polymer brushes have proven to be extraordinarily versatile platforms for the design of sensors,[5-10] the functionalization of biomaterials,[11-16] or the fabrication of lubricious surfaces[17-18] and catalytic supports,[19-22] the translation of SI-RDRP methods into technologically relevant surface-modification techniques still requires some intrinsic drawbacks to be overcome. These are mainly related to the low tolerance of SI-RDRP methods to oxygen,[23-24] which limits the scaling up of such grafting processes for large substrates, or those of diverse composition.

Focusing in particular on the most widely applied version of SI-RDRP, namely surface-initiated atom transfer radical polymerization (SI-ATRP),[25] the need for deoxygenation of monomer solutions has been recently circumvented by the introduction of reducing agents[26-28] or oxygen scavengers,[29] which consume oxygen that has diffused in from the surrounding environment, concomitantly regenerating the active catalyst or act as catalysts themselves,[30] ultimately enabling polymer grafting under ambient conditions.

Specifically, by exploiting activators regenerated by electron transfer (ARGET) ATRP, various waterborne monomers could be successfully polymerized from large polymeric films in the presence of oxygen,[31] while the application of photocatalysts in light-mediated, metal-free SI-ATRP enabled the fabrication of micropatterned brushes over entire silicon wafers, with high resolution and without the need for deoxygenation of reaction mixtures.[30]

Apart from the use of organic "additives" to improve the tolerance of SI-ATRP towards oxygen, Jordan et al. demonstrated that Cu^0-coated plates placed upon initiator-bearing substrates within polymerization mixtures could efficiently act as sources of catalyst,[32]

simultaneously consuming oxygen[33] and triggering the rapid growth of a variety of compositionally different brushes.[34] Apart from these initial findings, little has been uncovered concerning the mechanism of Cu^0-mediated SI-ATRP, and its tolerance towards oxygen, and its application has been limited to model, flat substrates.

While investigating the role played by the copper surface during Cu^0-mediated SI-ATRP (Cu^0 SI-ATRP) we recently demonstrated that the composition of the polymerization mixture and the separation between the Cu^0 surface and the initiator-bearing substrate represent key parameters that determine polymer-brush growth and its kinetics.[35-36]

In this study, we show that Cu^0 SI-ATRP enables the highly controlled synthesis of technologically relevant polymer brushes from large flat surfaces, as well as from different organic supports, including cellulose fibres and elastomers, by using microliter volumes of reaction mixtures—either under inert conditions or in the presence of oxygen. In particular, we systematically examine the parameters governing Cu^0 SI-ATRP, while focusing on the synthesis of poly(2-methacryloyloxyethyl phosphorylcholine) (PMPC) brushes, which have been widely applied for the fabrication of highly lubricious coatings[17-18, 37-39] and bio-repellent films.[40-44]

RESULTS AND DISCUSSION

Mechanism of Cu^0 SI-ATRP in Deoxygenated Media

The mechanism of Cu^0 SI-ATRP of MPC can be exemplarily investigated by placing a copper plate at 1 mm distance from an ATRP initiator-functionalized silicon oxide surface (Scheme 1), in the presence of a 1 M methanol solution of MPC and 40 mM of 2,2'-bipyridine (bipy). The growth of PMPC brushes is firstly investigated within deoxygenated reaction mixtures, while surrounding the reaction system with an N_2 atmosphere during the entire polymerization process. In the presence of organic ligand (L), Cu^I/L and Cu^{II}/L complexes diffuse from the

copper plate towards the initiator-bearing substrate, triggering the polymerization of MPC, which proceeds according to the ATRP equilibrium (Scheme 1).[36] The growth of PMPC brushes could be monitored ex situ by variable-angle spectroscopic ellipsometry (VASE), the dry brush thickness (T_{dry}) being determined for different polymerization times. As shown in Figure 1a, T_{dry} steady increased during the first 40 minutes of polymerization, reaching ~ 20 nm, after which a plateau was attained, indicating that the grafting process irreversibly stopped. This phenomenon was likely due to radical termination between growing grafts, as the concentration of Cu^{II}-based deactivator solely generated through the ATRP equilibrium at the growing-brush front was presumably insufficient to guarantee a low concentration of surface-grafted radicals.[36]

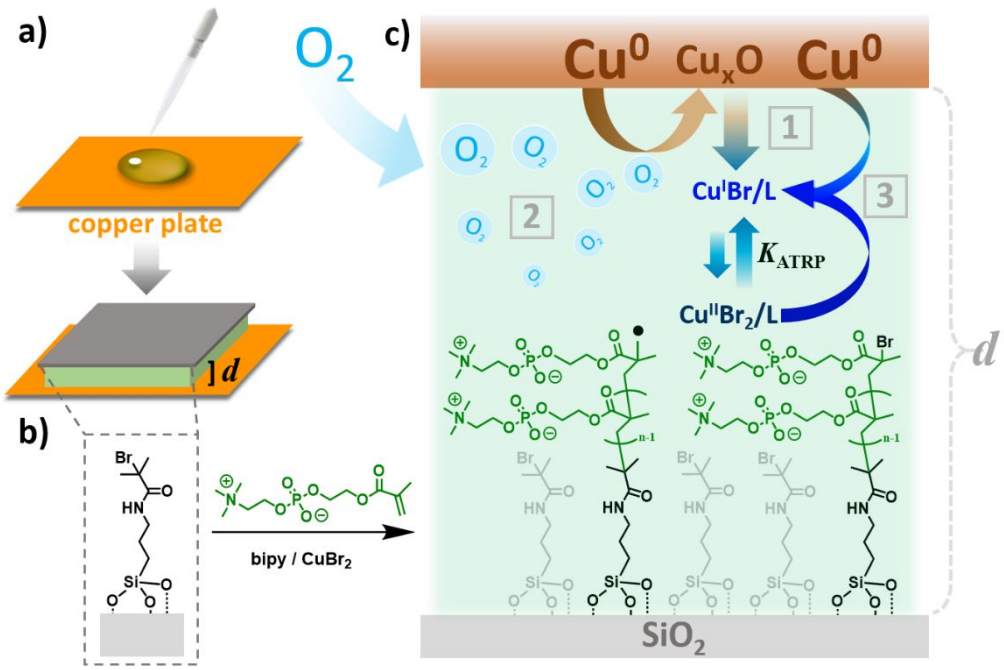

Scheme 1. Mechanism of Cu^0 SI-ATRP of MPC from ATRP-initiator-functionalized silicon oxide surfaces. (a,b) A polymerization solution (comprising 1 M methanol solution of MPC and 40 mM bipy, or 40 mM bipy and 0.2 mM $CuBr_2$) is sandwiched between a copper plate and an initiator-bearing substrate (c) When the solution has been previously degassed and the grafting process is carried out within an inert atmosphere, Cu^I/L and Cu^{II}/L species diffuse from the copper plate (1) and trigger MPC polymerization from the initiator-functionalized substrate, which proceeds according to the ATRP equilibrium. However, under ambient conditions and without previous deoxygenation of the reaction mixture, the dissolved oxygen is consumed by oxidation of Cu^0 (2), generating an oxide layer that acts as source of catalyst.

Either in the presence or the absence of oxygen, the addition of Cu^{II}-based species stimulates the formation of Cu^{I}/L activators through comproportionation with the Cu^0 surface (3).

The addition of 0.2 mM $CuBr_2$ to the reaction mixture substantially altered the growth kinetics of PMPC brushes. In the presence of added deactivator, the PMPC brush thickness continuously increased with reaction time, following a nearly linear trend, T_{dry} reaching nearly 70 nm after 75 minutes of polymerization (Figure 1a). On the one hand, the presence of additional Cu^{II}-based deactivator suppressed irreversible termination by radical recombination, ensuring the controlled growth of PMPC grafts. On the other hand, following a similar mechanism to that previously described for supplemental activator and reducing agent (SARA) ATRP,[45-47] Cu^{II} species comproportionated with the Cu^0 surface, constantly (re)generating Cu^{I}-based adducts capable of activating both dormant PMPC grafts and unreacted initiator functions at the surface (Scheme 1). The combination of these two cooperative effects led to the observed, highly controlled grafting of PMPC brushes.

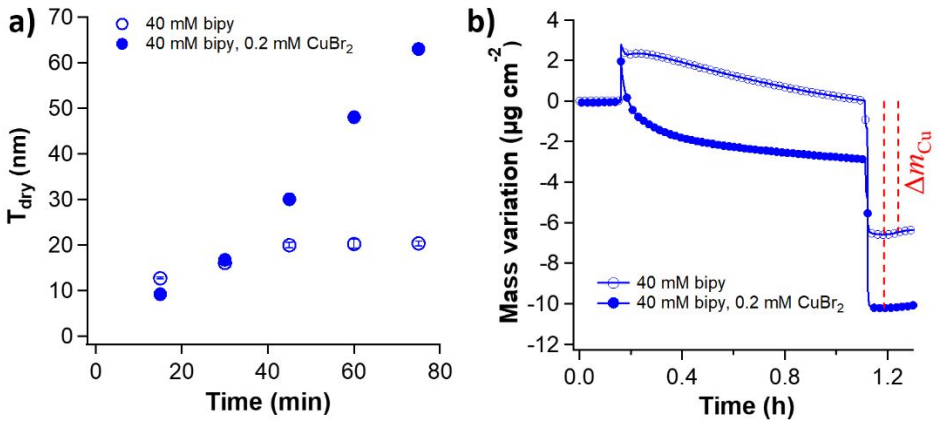

Figure 1. (a) PMPC brush dry thickness (T_{dry}) measured by VASE at different polymerization times, using a reaction mixture comprising either 1 M methanol solution of MPC and 40 mM bipy (empty markers), or 1 M MPC, 40 mM bipy and 0.2 mM $CuBr_2$ (filled markers). (b) Mass variation (Δm_{Cu}) of Cu^0-coated QCM-D sensors obtained from fitting of the corresponding frequency shifts (Δf) with the Sauerbrey equation (Supporting Information). The QCM-D sensors were subjected to different polymerization solutions: 1 M MPC and 40 mM bipy (empty markers), and 1 M MPC, 40 mM bipy and 0.2 mM $CuBr_2$ (filled markers).

Comproportionation between added Cu^{II} and the Cu^0 surface could be precisely monitored by means of a quartz crystal microbalance with dissipation (QCM-D), subjecting a Cu^0-coated QCM-D sensor to the same polymerization mixtures employed during Cu^0 SI-ATRP of MPC, while simultaneously monitoring the dissolution of copper species from the metal surface as a mass change in the copper-coated sensor (Δm_{Cu}). As highlighted in Figure 1b, the addition of 0.2 mM $CuBr_2$ caused a more marked desorption of Cu species from the metal-coated sensor, presumably mainly comprising Cu^I complexes generated by comproportionation, when compared to the mass loss measured when the sensor was in contact with a solution containing only ligand and monomer.

Structure and Properties of PMPC Brushes Synthesized by Cu^0 SI-ATRP

It is important to emphasize that the progressive brush thickening recorded by VASE was not simply due to an increase in the molar mass of PMPC grafts, but also to a simultaneous increment in their grafting density (σ). As Cu^I-based activators progressively diffuse from the Cu^0 surface towards and through the growing brush layer, an increasing number of initiators become activated, subsequently generating PMPC chains that propagate from the surface.

In order to support this hypothesis, we estimated the swelling ratio (SR) of PMPC brushes synthesized after different polymerization times by comparing the values of T_{dry} with the corresponding swollen brush thicknesses (T_{wet}), which could be measured by atomic force microscopy (AFM) nanoindentation (Experimental Methods and Figure S1). Since the SR of brushes in a good solvent is inversely proportional to σ,[48-50] its gradual decrease with the polymerization time from 5 to 1 (Figure 2a), indicated a simultaneous increment in brush surface coverage, which shifted from ~ 0.2 to ~ 0.7 chains nm^{-2}, between 15 and 75 minutes of polymerization.

This gradual change in brush structure was mirrored by a significant shift in other interfacial physicochemical properties. Besides the amount of swelling solvent, wettability progressively decreased due to the rising of inter- and intrachain ionic associations between zwitterions—a phenomenon that was previously reported for relatively thick and densely grafted sulfobetaine-based polyzwitterionic brushes, and which determined their more "hydrophobic" character with respect to thinner and less crowded brushes of identical composition (Figure 2a).[51] The formation of ionic "bridges" between PMPC brushes and the concomitant decrease in SR further influenced their lubrication properties, which were characterized by lateral force microscopy (LFM) (Experimental Methods).[52-53]

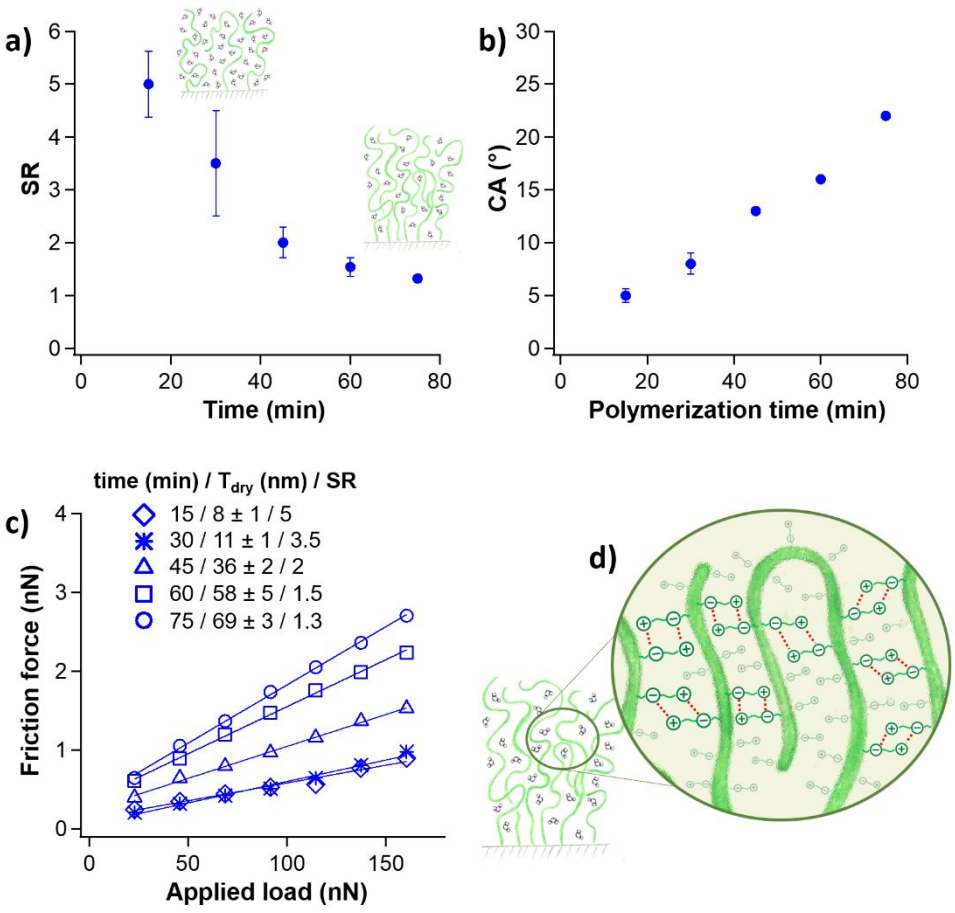

Figure 2. (a) Values of swelling ratio (SR) measured by a combination of VASE and AFM on PMPC brushes synthesized by Cu^0 SI-ATRP after different polymerization times under inert atmosphere ($SR = T_{wet}/T_{dry}$), using a reaction mixture comprising 1 M MPC, 40 mM bipy and 0.2 mM $CuBr_2$. (b) Static water contact angle (CA) measured on PMPC brushes synthesized

after different polymerization times, using the conditions reported in (a). (c) F_fL profiles recorded by LFM on PMPC brushes, using an AFM colloidal probe with a normal spring constant (K_N) of 0.3 N m^{-1}, a lateral spring constant (K_L) of 5.1 E-9 N m^{-1}, and an 18 μm diameter silica colloid. The coefficients of friction (μ) were 0.005, 0.005, 0.008, 0.012, and 0.015, measured on PMPC brushes synthesized after 15, 30, 45, 60, and 75 minutes, respectively. (d) Schematic representation of densely grafted PMPC brushes forming inter- and intrachain ionic associations.

As highlighted by comparing the friction-force-vs-applied-load (F_fL) profiles measured on PMPC brushes featuring different values of thickness (Figure 2b), friction was generally low, with coefficients of friction (μ) lying between 0.015 and 0.005, for 69 ± 3 and 8 ± 1 nm-thick brushes, respectively. However, a clear increase in the slope of F_fL profiles—and thus a consequent increment in μ—was observed with increasing the polymerization time, suggesting that the progressive structural transition taking place within PMPC brushes affected mechanical energy dissipation when these were sheared by an AFM colloidal probe.

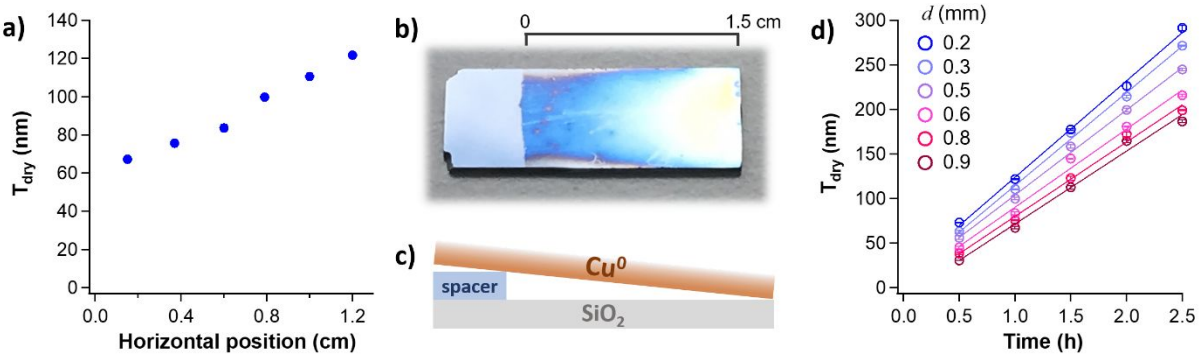

Figure 3. (a) Variation of T_{dry} across a PMPC brush gradient (b) synthesized by continuously varying the distance between a copper plate and an ATRP initiator-bearing substrate (c), in the presence of a polymerization mixture including a 1 M methanol solution of MPC, 40 mM bipy and 0.2 mM $CuBr_2$. The reaction mixture was deoxygenated by N_2 bubbling prior to Cu^0 SI-ATRP, while the brush gradient was fabricated over 1 hour of polymerization under a N_2 atmosphere. The rate of Cu^0 SI-ATRP, which correlated with the slope of the T_{dry} vs polymerization time profiles reported in (d), could be tuned by varying *d* between the copper plates and ATRP initiator-substrates.

The distance (*d*) between the copper plate and the initiator-bearing substrate represented an additional parameter governing the growth of PMPC brushes by Cu^0 SI-ATRP. When a continuous variation of *d* was applied across a single, initiator-functionalized substrate, by

"tilting" the copper plate (Figure 3a-c), the diffusion time for activator species gradually changed along the surface, and a PMPC brush-gradient was obtained.[35-36] In particular, in the presence of 0.2 mM $CuBr_2$ and after 1 hour of polymerization, the PMPC brush thickness progressively varied between 70 and 120 nm across a 1.5 cm-long substrate.

Alternatively, when the copper plate and the initiating surface were maintained parallel to each other, the rate of polymerization could be subsequently tuned by varying *d*, while keeping the other polymerization conditions constant. As reported in Figure 3d, polymer-brush-thickening rates increased with decreasing *d*, and the thickness of PMPC brushes synthesized after 2,5 hours of Cu^0 SI-ATRP could be varied from ~ 180 to almost 300 nm by reducing the distance to the copper plate from 0.9 to 0.2 mm (Figure 3d).

Functionalization of Large and Compositionally Different Substrates by Cu^0 SI-ATRP under Ambient Conditions

Cu^0 SI-ATRP of MPC performed without deoxygenation of monomer mixtures and under ambient conditions followed a very similar mechanism to that observed for oxygen-free polymerizations carried out within an inert atmosphere.

When the reaction mixture is sandwiched between the copper plate and the initiator-functionalized substrate, while a constant pressure of 3 g cm^{-2} is applied, the distance between the two surfaces corresponds to ~ 10 μm. Under these conditions, the area of air-liquid interface at the edges of the overlying substrates is small enough to guarantee limited diffusion of oxygen from the surrounding atmosphere (Scheme 1c). The Cu^0 surface consumes the oxygen dissolved in the reaction mixture, generating a CuO_x layer that acts as source of catalyst. In the presence of L, Cu^I/L and Cu^{II}/L species diffuse to the initiating surface and trigger the grafting of PMPC brushes, which proceeds according to the ATRP process.

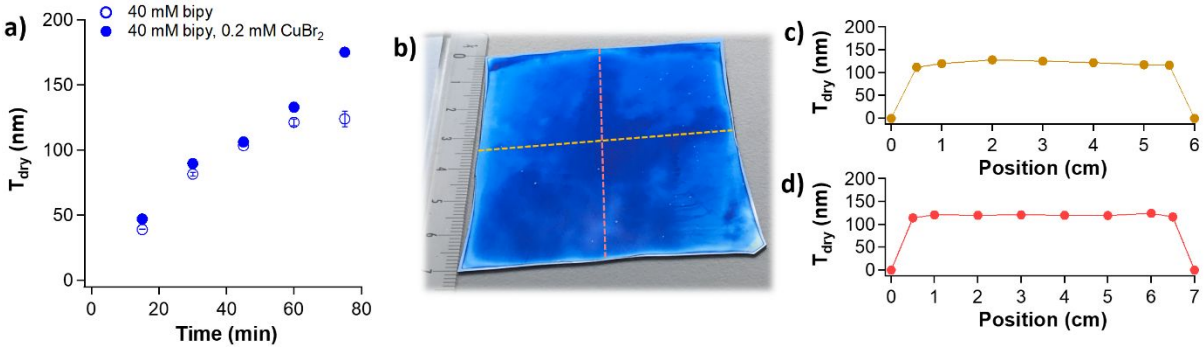

Figure 4. (a) Cu^0 SI-ATRP of MPC performed without deoxygenation of monomer mixtures and under ambient conditions, using 1 M methanol solution of MPC and 40 mM bipy (empty markers), or 40 mM bipy and 0.2 mM $CuBr_2$ (filled markers). During these experiments, *d* was kept at 10 μm by applying a constant pressure of 3 g cm^{-2} on the sandwiched assembly. (b) PMPC brushes synthesized by Cu^0 SI-ATRP in the presence of oxygen from ~ 50 cm^2 silicon oxide substrate previously functionalized with ATRP initiator and covered by a copper plate with d = 10 μm. By using a polymerization mixture comprising 1 M MPC, 40 mM bipy and 0.2 mM $CuBr_2$ uniform PMPC brushes with a dry thickness of ~ 120 nm were synthesized after 60 minutes of reaction. (c,d) Brush-thickness profiles recorded by VASE across the large substrate reported in (b).

Similarly to what was previously observed while using deoxygenated mixtures and an inert atmosphere, the addition of Cu^{II} strongly influenced the growth kinetics of PMPC brushes by Cu^0 SI-ATRP in the presence of oxygen. As shown in Figure 4a, in the absence of externally added Cu^{II}, PMPC brush growth proceeded steadily during the first 60 minutes of polymerization until ~ 100 nm of film thickness was reached. After this time, the brush-thickening rate slowed down and reached a plateau, presumably due to irreversible termination by radical combination/disproportionation.

In contrast, the addition of 0.2 mM $CuBr_2$ enabled a progressive brush growth, which followed a *quasi*-linear trend and indicated rapid and highly controlled polymerization. Under these conditions, ~ 130 nm-thick PMPC brushes could be synthesized in just 60 minutes of polymerization, while no sign of termination was observed.

Following this procedure, homogeneously thick PMPC brushes could be grown from large substrates, after just 1 hour of polymerization, without the need for degassing monomer mixtures, and by employing just 8 μL cm^{-2} of polymerization solution.

An example of the applicability of Cu^0 SI-ATRP for the functionalization of large substrates under full ambient conditions is provided in Figure 4b, which shows 120-nm-thick PMPC brushes grafted from a 50 cm^2 silicon substrate. PMPC brush thickness was homogenous across the entire surface (Figure 4c and 4d), with the exception of its edges, where unavoidable oxygen diffusion terminated the polymerization, resulting in a localized reduction in film thickness.

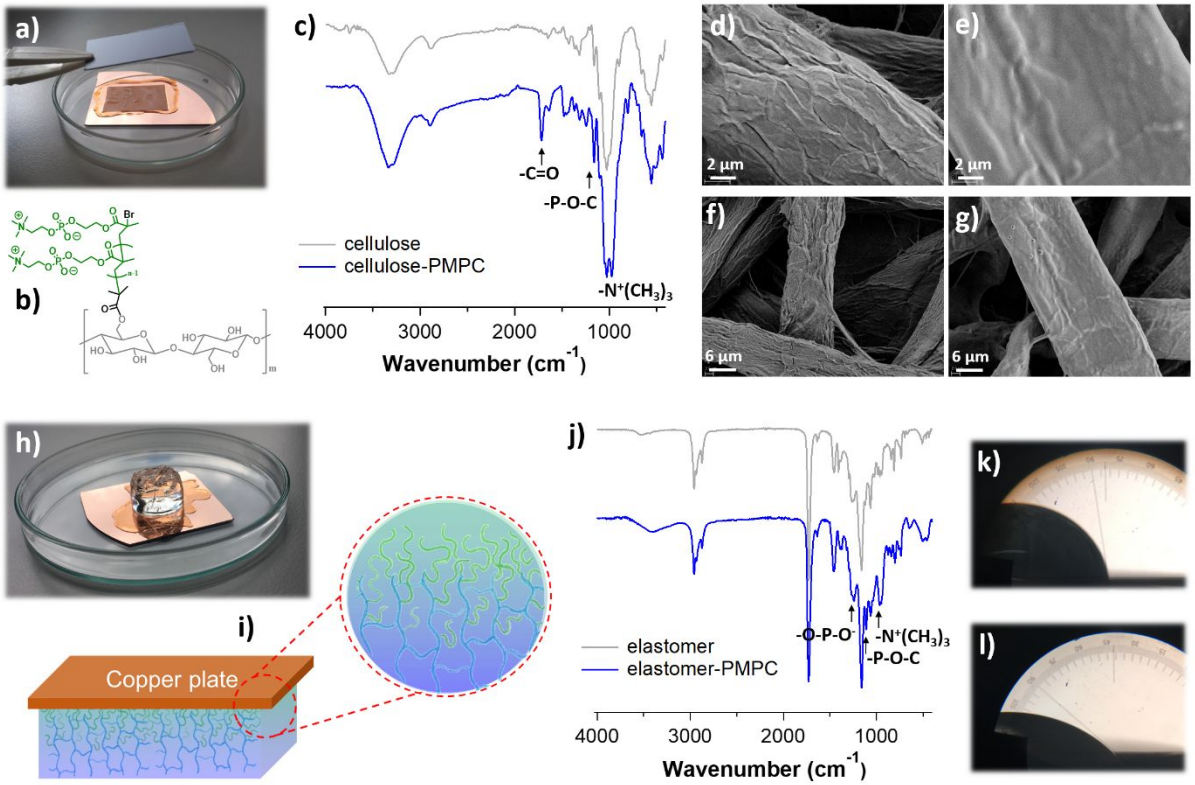

Figure 5. (a, b) Uniform PMPC brush-films can be successfully grown from cellulose sheets previously functionalized with ATRP initiator functions (Supporting Information) by Cu^0 SI-ATRP in the presence of oxygen. The reaction mixture comprised 1 M methanol solution of MPC, 40 mM bipy and 0.2 mM $CuBr_2$ and the polymerization time was set to 1 hour. (c) Attenuated total reflectance Fourier-transform infrared spectroscopy (ATR FTIR) confirmed the successful grafting of PMPC brushes, SEM further demonstrated the formation of an uniform PMPC brush film on cellulose fibres (d-g). Cu^0 SI-ATRP can be further applied for the modification of the outer surface of a PBA-based elastomer, by placing the stamp in contact with a copper plate previously covered by few drops of reaction mixture (h,i). The formation of PMPC brushes was confirmed by ATR FTIR spectroscopy (j) and wettability measurements (k, l).

In order to further demonstrate the suitability of Cu^0 SI-ATRP for the rapid and efficient modification of a variety of materials, beyond flat, model substrates, similar PMPC brushes were subsequently grafted from micro- and nanoporous supports, including cellulose sheets and poly(butyl acrylate) (PBA)-based elastomers (Figure 5 and Figure S5). It is noteworthy that structurally similar supports are widely applied for the fabrication of medical devices, such as wound dressings and catheters, where the highly hydrophilic, biopassive and lubricious properties of PMPC brushes[18, 41, 43-44, 54-55] could substantially improve their performance when placed in contact with tissues and/or body fluids.

When microporous cellulose sheets previously derivatised by ATRP initiator functions (Experimental Methods) and soaked with few tens of μL of monomer mixture were sandwiched between an inert silicon substrate and a copper plate, thick PMPC brushes were successfully grown in 60 minutes of reaction (Figure 5a and 5b), as evidenced by a combination of attenuated total reflectance Fourier-transform infrared spectroscopy (ATR FTIR) and scanning electron microscopy (SEM). In particular, ATR FTIR confirmed the successful grafting of PMPC brushes, through the appearance of the signal at 1730 cm^{-1}, corresponding to C=O stretching in the polymer repeating unit, the band centered at 1240 cm^{-1}, corresponding to -O-P-O^-, and that at 970 cm^{-1} referring to -$N^+(CH_3)_3$ (Figure 5c). SEM further demonstrated the formation of an uniform PMPC brush film on cellulose fibres, by comparing the micrographs recorded on pristine sheets (Figure 5d and 5f) with those obtained after Cu^0 SI-ATRP of MPC (Figure 5e and 5g).

Alternatively, Cu^0 SI-ATRP could be applied for the modification of the exposed surface of a PBA-based elastomer, where uniform PMPC brushes were grafted by simply placing the elastomeric stamp in contact with a copper plate, which was previously covered by few drops of polymerization solution. Also in this case, the reaction mixture was not deoxygenated, and the modification of the elastomer was performed without the presence an inert atmosphere, but

simply on a petri dish exposed to air. After 1 hour of polymerization, the growth of PMPC brushes was confirmed by ATR FTIR spectroscopy (Figure 5j), through the appearance of the signals at 1240 cm^{-1} (-O-P-O$^-$), 1080 cm^{-1} (-P-O-C), and 970 cm^{-1} (-$N^+(CH_3)_3$), characteristic of the PMPC repeating unit. Wettability measurements further demonstrated the formation of a hydrophilic PMPC film on the elastomer, the static water contact angle (CA) shifting from 83 ± 2° (Figure 5k) to 40 ± 1° (Figure 5l).

CONCLUSIONS

Cu^0 SI-ATRP has been demonstrated to be an efficient, highly versatile and extremely controlled grafting technique, which is compatible with flat inorganic surfaces, as well as with porous organic supports of different compositions. The intrinsically confined nature of Cu^0 SI-ATRP, which exploits the intimate contact between a copper plate, acting as source of catalyst and reducing agent, and an initiator-bearing support, determines its many attractive features. This process enables the rapid growth of technologically relevant polymer brushes, over very large and morphologically different substrates, using microliter volumes of reaction mixtures, and without the need for their deoxygenation or an inert atmosphere. These unique characteristics, which were highlighted here for the case of the synthesis of PMPC brushes, demonstrate that the application of Cu^0 SI-ATRP for surface modification can translate SI-RDRP methods from academic studies into technology, opening a plethora of possible applications in materials science.

EXPERIMENTAL METHODS

Materials. Silicon wafers were purchased from Si-Mat (P/B ⟨100⟩, Si-Mat Silicon Wafers, Landsberg, Germany). Copper plates were obtained by coating silicon wafers with 200 nm of Cu^0 by magnetron sputtering (Paul Scherrer Institute, Villigen, Switzerland).

3-(Aminopropyl)triethoxysilane (APTES, 99%, Acros), 2-bromoisobutryl bromide (BiBB, 98%, Sigma-Aldrich), triethylamine (TEA, ≥99%, Merck), dichloromethane (DCM, dry, ≥99.8%, Acros), 2-methacryloyloxyethyl phosphorylcholine (MPC, 97%, Sigma-Aldrich), methanol (> 99%, VWR Chemicals), 2,2'-bipyridine (>=99%, Sigma-Aldrich), diphenyl(2,4,6-trimethylbenzoyl)phosphine oxide (TPO, Sigma-Aldrich, 97%), 2-methacryloyloxyethyl phosphorylcholine (MPC, Sigma-Aldrich, 97%), and copper(II) bromide ($CuBr_2$, 99.99%, Aldrich) were used as received. Butyl acrylate (BA, 99%, Acros Organics), hydroxyethylmethacrylate (HEMA, 98%, Sigma-Aldrich) and poly(ethylene glycol) dimethacrylate (PEGDMA, M_n ~ 550) were purified from inhibitors by filtration through a basic alumina column. All the other chemicals were purchased from Sigma-Aldrich. Water used in all the experiments was Millipore Milli-Q grade.

Quartz Crystal Microbalance with Dissipation (QCM-D). QCM-D was used to monitor the dissolution of Cu species from Cu^0-coated sensors, when immersed in different polymerization mixtures, using an E4 instrument (Q-Sense AB, Göteborg, Sweden) equipped with dedicated Q-Sense AB software. Cu-coated crystals (LOT-Oriel AG) with a fundamental resonance frequency of 5 MHz were used as substrates. Before the experiment, the sensors were cleaned by 15 minutes sonication in toluene and 2-propanol, and finally immersed in a 2:1 v/v mixture of methanol and 37% HCl, in order to remove Cu_xO layer. After cleaning, the crystals were dried under a stream of N_2. In order to measure the desorption of Cu species, Cu^0-coated sensors were mounted in the QCM-D chamber and subsequently subjected to different polymerization mixtures. The recorded frequency shift (Δf) was correlated to the decrease of mass of the Cu layer on the sensor, by applying the Sauerbrey relation,[56] using the sensitivity factor $C_f = -17.7$ ng Hz^{-1} cm^{-2}.

Variable-Angle Spectroscopic Ellipsometer (VASE). The values of dry thickness of the different brush films (T_{dry}) were measured using a M-2000F Woollam variable angle

spectroscopic ellipsometer (J.A. Woollam Co. U.S.). The values of Ψ and Δ were acquired as a function of wavelength (275−827 nm) using focusing lenses at 70 ° from the surface normal. Fitting of the raw data was performed based on a three-layer model, using bulk dielectric functions for Si, and SiO_2. The polymer brush layers were analyzed on the basis of the Cauchy model: $n = A + B \lambda^{-2}$, where n is the refractive index, λ is the wavelength and A and B were assumed to be 1.45 and 0.01, respectively, as values for transparent organic films.[57]

Atom Force Microscopy (AFM). Force-vs-separation (FS) analysis and lateral force microscopy (LFM) on PMPC brushes was performed using a MFP3D AFM (Asylum Research, Oxford Instruments, Santa Barbara, USA) under 10 mM of 4-(2-hydroxyethyl)-1-piperazine-1-ethane- sulfonic acid (HEPES) buffer (pH = 7.4). The normal (K_N) and torsional spring (K_T) constants of tipless cantilevers were measured by the thermal-noise[58] and Sader's method,[59] respectively, resulting $K_N = 0.296$ N m^{-1} and $K_T = 5.1\ E^{-9}$ N m. The "wall method" reported by Cannara et al.,[60] was used for calibration of friction force.

Silica microspheres (EKA Chemicals AM, Kormasil) having a diameter of 18 μm were glued to the end of the calibrated cantilevers by a home-built micromanipulator, using an epoxy glue (Araldite® Standard). The cantilevers were cleaned by UV-ozone treatment for 30 min prior to the measurements.

Friction values were obtained by averaging 10 "friction loops" recorded on each brush surface over three different positions for each sample. The friction loops were acquired by laterally scanning over a line on each brush film at a given applied normal load. A scanning distance of 5 μm and a scanning rate of 1 Hz were applied during the measurements. The values of coefficient of friction (μ) were obtained from the slope of the recorded friction force-vs-applied load ($F_f L$) profiles, assuming the Amontons law of friction: $F_f = \mu L$.

Approximately 20 FS profiles were recorded on each PMPC brush by applying a Z-piezo distance of 500 nm and a ramping rate of 1 Hz (Figure S1). The swollen thickness of the brushes

(T_{wet}) was obtained by estimating the separation included between the contact point at the brush interface (in correspondence of which the measured force deviates by more than 5% from the horizontal line corresponding to F = 0 nN) and the complete brush compression (Figure S1). From the values of T_{dry}, obtained by VASE, and those of T_{wet}, the brush swelling ratio (SR) could be calculated as T_{wet}/T_{dry}. The grafting density (σ) of PMPC brushes was estimated according to the previously reported method, using Equation 1:[36, 48-50]

$$\sigma = \rho_0 T_{dry} N_A \left((0.227\,(T_{wet})^{1.5}\left(T_{dry}\,(Å^2)\right)^{-0.5})M_0\right)^{-1} \quad (1)$$

where ρ_0 is the dry density of PMPC (1.30 g cm^{-3}), N_A is Avogadro's number, M_0 is the monomer molecular weight (295 g mol^{-1}), 0.227 is a constant related to the excluded volume parameter (ω =7 $Å^3$), a constant $v = (a^2/3)^{-1}$, where a represents the Kuhn length of the monomer unit (15 Å for methyl methacrylate).

Water-Contact-Angle Measurements. A Ramé-Hart goniometer (model-100, Netcong, NJ) was used to measure the static water contact angle (CA) on the different PMPC brush surfaces. Three individual measurements were performed with a drop-shape analysis system at room temperature. The contact-angle values were obtained by using the tangent-fitting method.

ATRP Initiator-Functionalized Silicon Oxide Substrates. Silicon wafers used as substrates for Cu^0 SI-ATRP were cleaned for 30 minutes in "piranha" solution (3:1 v/v mixture of 99.9% H_2SO_4 and H_2O_2, CAUTION: piranha solutions react violently with organic compounds, and may result in explosion or skin burns if not handled with extreme caution), and subsequently rinsed with ultrapure water and ethanol. ATRP initiator layers were subsequently deposited using a two-steps protocol. APTES was first immobilized through vapour deposition during 3 hours. After this, the substrates were incubated for 2 hours in a dichloromethane solution of BiBB and TEA, subsequently washed with chloroform and dried under a stream of N_2.

Cu^0 SI-ATRP Using Deoxygenated Reaction Mixtures. In order to fabricate PMPC brushes with homogeneous thickness ATRP-bearing initiator substrates were clamped to Cu^0-coated

surfaces while maintaining a fixed distance (*d*) of 1 mm between the two surfaces, by means of a glass slide (Figure S2). PMPC brush gradients were prepared with a similar setup, but by tilting the ATRP initiator-bearing surface with respect to the Cu^0-coated substrate, as depicted in Figure S2. The clamped substrates were laid in a sealed flask and degassed with Ar for 30 min. A degassed methanol mixture of MPC (1M) and bipy (40 mM), with and without $CuBr_2$ (0.2mM), was transferred into the flask containing the substrates, and left standing for the desired time. After this, the samples were rinsed extensively with water and ethanol and finally dried in a stream of N_2.

Cu^0 SI-ATRP of MPC under Ambient Conditions. Cu^0-coated substrates were washed with isopropanol under sonication (5 min), followed by activation protocol in a 2:1 v/v mixture of methanol and 37% HCl. A polymerization mixture including MPC (1 M), bipy (40 mM), with or without $CuBr_2$ (0.2 mM) was dropped on the activated Cu^0 surface, and immediately covered with ATRP initiator-functionalized substrate, while a constant pressure of 3 g cm^{-2} was applied between the sandwiched substrates. The volume of the polymerization mixture applied was 8 μL cm^{-2}. After the desired polymerization time, the substrates were thoroughly washed with water and ethanol and dried in a stream of N_2.

Functionalization of Cellulose Sheets with ATRP Initiator. Cellulose sheets were functionalized with ATRP initiator using the already reported method.[61] Cellulose sheets were washed with acetone and tetrahydrofuran (THF) and subsequently immersed in a mixture containing BiBB (230 mg, 1.0 mmol, 50 mM), TEA (111 mg, 1.1 mmol, 55 mM), and a catalytic amount of DMAP in THF (20 mL). The reaction was conducted for 2 hours, after which the cellulose substrates were washed with dichloromethane and methanol thoroughly, and dried under N_2 stream.

Cu^0 SI-ATRP from Cellulose Sheets. 50 μL of a solution of MPC (1M), bipy (40 mM), and $CuBr_2$ (0.2 mM) was poured on a cellulose sheer previously placed on a Cu^0-coated substrate,

and immediately covered by a freshly cleaned silicon substrate. After the desired polymerization time, the reaction was terminated by rinsing the filter paper with water and methanol and dried under a stream of N_2. The modified cellulose sheet was subsequently analyzed by attenuated total reflectance Fourier-transform infrared spectroscopy (ATR-FTIR) and SEM.

Synthesis of PBA-Based Elastomers. PBA-based elastomers were synthesized via photo-initiated radical polymerization (Figure S5). Mixtures including butyl acrylate (0.153 mol, 4.78 M), HEMA (0.016 mol, 0.5 M) and PEGDMA (1.69 mmol, 52.8 mM) were degassed in 10 ml toluene for 20 min, after that, TPO (0.2 mM in toluene) was added. The polymerization was conducted under UV light (λ = 365 nm, 1.2 mW cm^{-2}) using a Stratalinker UV crosslinker 2400 (Stratagene, La Jolla, CA, USA) at room temperature for 60 min. PBA elastomers were de-moulded from reaction vials, followed by washing thoroughly with toluene. ATRP initiators were generated on PBA-based elastomers by vapour deposition of BiBB (Figure S5), followed by rinsing with chloroform and toluene.

Cu^0 SI-ATRP from PBA-Based Elastomers. 0.5 mL of a polymerization solution including MPC (1M), bipy (40 mM), and $CuBr_2$ (0.2 mM) were poured on a previously activated Cu^0-coated substrate and immediately covered with an ATRP-initiator functionalized PBA-based elastomer. After the desired polymerization time, the sample was rinsed with methanol and water, and finally dried under a stream of N_2. Elastomers presenting PMPC brushes were subsequently analyzed by ATR-FTIR and CA.

Scanning Electron Microscope (SEM). PMPC brush-functionalized cellulose sheets were sputter coated (CCU-010 Compact coating unit; Safematic) with 3 nm of platinum, in order to avoid surface charging during imaging. A scanning electron microscope (SEM, Thermo scientific, ultradry) equipped with a LEO 1530 operating instrument (Zeiss GmbH, Germany), was used to record the micrographs.

Associated Content

Supporting Information. Further AFM characterizations and additional details regarding experimental methods are provided on the ACS publication website at DOI: XXX

Author Information

Corresponding Authors:

*Email: nicholas.spencer@mat.ethz.ch

*Email: matyjaszewski@cmu.edu

*Email: edmondo.benetti@mat.ethz.ch

Acknowledgments

This work was financially supported by European Union's Horizon 2020 research and innovation program (grant agreement No 669562), the Swiss National Science Foundation (SNSF "Ambizione" PZ00P2−790 148156), and the National Science Foundation (DMR 1501324).

Competing interests

The authors declare no competing interests.

References

1. Zoppe, J. O.; Ataman, N. C.; Mocny, P.; Wang, J.; Moraes, J.; Klok, H. A., Surface-Initiated Controlled Radical Polymerization: State-of-the-Art, Opportunities, and Challenges in Surface and Interface Engineering with Polymer Brushes (vol 117, pg 1105, 2017). *Chem. Rev.* **2017,** *117* (5), 4667-4667.

2. Barbey, R.; Lavanant, L.; Paripovic, D.; Schuwer, N.; Sugnaux, C.; Tugulu, S.; Klok, H. A., Polymer Brushes via Surface-Initiated Controlled Radical Polymerization: Synthesis, Characterization, Properties, and Applications. *Chem. Re.v* **2009,** *109* (11), 5437-5527.
3. Omar, A., Polymer Brushes Here, There, and Everywhere: Recent Advances in Their Practical Applications and Emerging Opportunities in Multiple Research Fields. *J. Polym. Sci. A* **2012,** *50* (16), 3225-3258.
4. Chen, W.-L.; Cordero, R.; Tran, H.; Ober, C. K., 50th Anniversary Perspective: Polymer Brushes: Novel Surfaces for Future Materials. *Macromolecules* **2017,** *50* (11), 4089-4113.
5. Zhou, F.; Shu, W. M.; Welland, M. E.; Huck, W. T. S., Highly Reversible and Multi-Stage Cantilever Actuation Driven by Polyelectrolyte Brushes. *J. Am. Chem. Soc.* **2006,** *128* (16), 5326-5327.
6. Joh, D. Y.; Hucknall, A. M.; Wei, Q. S.; Mason, K. A.; Lund, M. L.; Fontes, C. M.; Hill, R. T.; Blair, R.; Zimmers, Z.; Achar, R. K.; Tseng, D.; Gordan, R.; Freemark, M.; Ozcan, A.; Chilkoti, A., Inkjet-Printed Point-of-Care Immunoassay on a Nanoscale Polymer Brush Enables Subpicomolar Detection of Analytes in Blood. *Proc. Natl. Acad. Sci. U.S.A.* **2017,** *114* (34), E7054-E7062.
7. Badoux, M.; Billing, M.; Klok, H. A., Polymer Brush Interfaces for Protein Biosensing Prepared by Surface-Initiated Controlled Radical Polymerization. *Polym. Chem.* **2019**, 10, 2925-2951
8. Fortin, N.; Klok, H. A., Glucose Monitoring Using a Polymer Brush Modified Polypropylene Hollow Fiber-based Hydraulic Flow Sensor. *ACS Appl. Mater. Interfaces* **2015,** *7* (8), 4631-4640.
9. Benetti, E. M.; Acikgoz, C.; Sui, X. F.; Vratzov, B.; Hempenius, M. A.; Huskens, J.; Vancso, G. J., Nanostructured Polymer Brushes by UV-Assisted Imprint Lithography and Surface-Initiated Polymerization for Biological Functions. *Adv. Funct. Mater.* **2011,** *21* (11), 2088-2095.
10. Christau, S.; Genzer, J.; von Klitzing, R., Polymer Brush/Metal Nanoparticle Hybrids for Optical Sensor Applications: from Self-Assembly to Tailored Functions and Nanoengineering. *Z. Phys. Chem.* **2015,** *229* (7-8), 1089-1117.
11. Gautrot, J. E.; Wang, C.; Liu, X.; Goldie, S. J.; Trappmann, B.; Huck, W. T.; Watt, F. M., Mimicking Normal Tissue Architecture and Perturbation in Cancer with Engineered Micro-Epidermis. *Biomaterials* **2012,** *33* (21), 5221-5229.
12. Desseaux, S.; Klok, H. A., Fibroblast adhesion on ECM-Derived Peptide Modified Poly(2-hydroxyethyl methacrylate) Brushes: Ligand Co-Presentation and 3D-Localization. *Biomaterials* **2015,** *44*, 24-35.
13. Desseaux, S.; Klok, H.-A., Temperature-Controlled Masking/Unmasking of Cell-Adhesive Cues with Poly(ethylene glycol) Methacrylate Based Brushes. *Biomacromolecules* **2014,** *15*, 3859-65.
14. Paripovic, D.; Hall-Bozic, H.; Klok, H. A., Osteoconductive Surfaces Generated from Peptide Functionalized Poly(2-hydroxyethyl methacrylate-co-2-(methacryloyloxy)ethyl phosphate) Brushes. *J. Mater. Chem.* **2012,** *22* (37), 19570-19578.
15. Raynor, J. E.; Petrie, T. A.; Garcia, A. J.; Collard, D. M., Controlling Cell Adhesion to Titanium: Functionalization of Poly[oligo(ethylene glycol)methacrylate] Brushes with Cell-Adhesive Peptides. *Adv. Mater.* **2007,** *19* (13), 1724-1728.
16. Klein Gunnewiek, M.; Di Luca, A.; Bollemaat, H. Z.; van Blitterswijk, C. A.; Vancso, G. J.; Moroni, L.; Benetti, E. M., Creeping Proteins in Microporous Structures: Polymer

Brush-Assisted Fabrication of 3D Gradients for Tissue Engineering. *Adv. Health. Mater.* **2015,** *4* (8), 1169–1174.

17. Zhang, Z. Y.; Morse, A. J.; Armes, S. P.; Lewis, A. L.; Geoghegan, M.; Leggett, G. J., Effect of Brush Thickness and Solvent Composition on the Friction Force Response of Poly(2-(methacryloyloxy)ethylphosphorylcholine) Brushes. *Langmuir* **2011,** *27* (6), 2514-2521.
18. Kobayashi, M.; Terayama, Y.; Hosaka, N.; Kaido, M.; Suzuki, A.; Yamada, N.; Torikai, N.; Ishihara, K.; Takahara, A., Friction Behavior of High-Density Poly(2-methacryloyloxyethyl phosphorylcholine) Brush in Aqueous Media. *Soft Matter* **2007,** *3* (6), 740-746.
19. Rafti, M.; Brunsen, A.; Fuertes, M. C.; Azzaroni, O.; Soler-Illia, G. J. A. A., Heterogeneous Catalytic Activity of Platinum Nanoparticles Hosted in Mesoporous Silica Thin Films Modified with Polyelectrolyte Brushes. *ACS Appl. Mater. Interfaces* **2013,** *5* (18), 8833-8840.
20. Benetti, E. M., Quasi-3D-Structured Interfaces by Polymer Brushes. *Macromol. Rapid Commun.* **2018,** *39* (14).
21. Costantini, F.; Benetti, E. M.; Tiggelaar, R. M.; Gardeniers, H. J. G. E.; Reinhoudt, D. N.; Huskens, J.; Vancso, G. J.; Verboom, W., A Brush-Gel/Metal-Nanoparticle Hybrid Film as an Efficient Supported Catalyst in Glass Microreactors. *Chem. Eur. J.* **2010,** *16* (41), 12406-12411.
22. Costantini, F.; Benetti, E. M.; Reinhoudt, D. N.; Huskens, J.; Vancso, G. J.; Verboom, W., Enzyme-Functionalized Polymer Brush Films on the Inner Wall of Silicon-Glass Microreactors with Tunable Biocatalytic Activity. *Lab. Chip* **2010,** *10* (24), 3407-3412.
23. Yeow, J.; Chapman, R.; Gormley, A. J.; Boyer, C., Up in the Air: Oxygen Tolerance in Controlled/Living Radical Polymerisation. *Chem. Soc. Rev.* **2018,** *47* (12), 4357-4387.
24. Li, M.; Fromel, M.; Ranaweera, D.; Rocha, S.; Boyer, C.; Pester, C. W., SI-PET-RAFT: Surface-Initiated Photoinduced Electron Transfer-Reversible Addition–Fragmentation Chain Transfer Polymerization. *ACS Macro Lett.* **2019,** *8*, 374-380.
25. Matyjaszewski, K.; Miller, P. J.; Shukla, N.; Immaraporn, B.; Gelman, A.; Luokala, B. B.; Siclovan, T. M.; Kickelbick, G.; Vallant, T.; Hoffmann, H.; Pakula, T., Polymers at Interfaces: Using Atom Transfer Radical Polymerization in the Controlled Growth of Homopolymers and Block Copolymers from Silicon Surfaces in the Absence of Untethered Sacrificial Initiator. *Macromolecules* **1999,** *32* (26), 8716-8724.
26. Matyjaszewski, K.; Dong, H. C.; Jakubowski, W.; Pietrasik, J.; Kusumo, A., Grafting from Surfaces for "Everyone": ARGET ATRP in the Presence of Air. *Langmuir* **2007,** *23* (8), 4528-4531.
27. Dunderdale, G. J.; England, M. W.; Urata, C.; Hozumi, A., Polymer Brush Surfaces Showing Superhydrophobicity and Air-Bubble Repellency in a Variety of Organic Liquids. *ACS Appl. Mater. Interfaces* **2015,** *7* (22), 12220-12229.
28. Dunderdale, G. J.; Urata, C.; Miranda, D. F.; Hozumi, A., Large-Scale and Environmentally Friendly Synthesis of pH-Responsive Oil-Repellent Polymer Brush Surfaces under Ambient Conditions. *ACS Appl. Mater. Interfaces* **2014,** *6* (15), 11864-11868.
29. Navarro, L. A.; Enciso, A. E.; Matyjaszewski, K.; Zauscher, S., Enzymatically Degassed Surface-Initiated Atom Transfer Radical Polymerization with Real-Time Monitoring. *J. Am. Chem. Soc.* **2019,** *141* (7), 3100-3109.
30. Narupai, B.; Page, Z. A.; Treat, N. J.; McGrath, A. J.; Pester, C. W.; Discekici, E. H.; Dolinski, N. D.; Meyers, G. F.; de Alaniz, J. R.; Hawker, C. J., Simultaneous Preparation of Multiple Polymer Brushes under Ambient Conditions using Microliter Volumes. *Angew. Chem. Int. Edit.* **2018,** *57* (41), 13433-13438.

31. Sato, T.; Dunderdale, G. J.; Urata, C.; Hozumi, A., Sol-Gel Preparation of Initiator Layers for Surface-Initiated ATRP: Large-Scale Formation of Polymer Brushes Is Not a Dream. *Macromolecules* **2018,** *51* (24), 10065-10073.
32. Zhang, T.; Du, Y. H.; Muller, F.; Amin, I.; Jordan, R., Surface-Initiated Cu(0) Mediated Controlled Radical Polymerization (SI-CuCRP) Using a Copper Plate. *Polym. Chem.* **2015,** *6* (14), 2726-2733.
33. Zhang, T.; Du, Y. H.; Kalbacova, J.; Schubel, R.; Rodriguez, R. D.; Chen, T.; Zahn, D. R. T.; Jordan, R., Wafer-Scale Synthesis of Defined Polymer Brushes under Ambient Conditions. *Polym. Chem.* **2015,** *6* (47), 8176-8183.
34. Zhang, T.; Benetti, E. M.; Jordan, R., Surface-Initiated Cu(0)-Mediated CRP for the Rapid and Controlled Synthesis of Quasi-3D Structured Polymer Brushes. *ACS Macro Lett.* **2019,** *8* (2), 145-153.
35. Dehghani, E. S.; Du, Y.; Zhang, T.; Ramakrishna, S. N.; Spencer, N. D.; Jordan, R.; Benetti, E. M., Fabrication and Interfacial Properties of Polymer Brush Gradients by Surface-Initiated Cu(0)-Mediated Controlled Radical Polymerization. *Macromolecules* **2017,** *50* (6), 2436-2446.
36. Fantin, M.; Ramakrishna, S. N.; Yan, J. J.; Yan, W. Q.; Divandari, M.; Spencer, N. D.; Matyjaszewski, K.; Benetti, E. M., The Role of Cu^0 in Surface-Initiated Atom Transfer Radical Polymerization: Tuning Catalyst Dissolution for Tailoring Polymer Interfaces. *Macromolecules* **2018,** *51* (17), 6825-6835.
37. Zhang, Z. Y.; Morse, A. J.; Armes, S. P.; Lewis, A. L.; Geoghegan, M.; Leggett, G. J., Nanoscale Contact Mechanics of Biocompatible Polyzwitterionic Brushes. *Langmuir* **2013,** *29* (34), 10684-10692.
38. Tairy, O.; Kampf, N.; Driver, M. J.; Armes, S. P.; Klein, J., Dense, Highly Hydrated Polymer Brushes via Modified Atom-Transfer-Radical-Polymerization: Structure, Surface Interactions, and Frictional Dissipation. *Macromolecules* **2015,** *48* (1), 140-151.
39. Chen, M.; Briscoe, W. H.; Armes, S. P.; Klein, J., Lubrication at Physiological Pressures by Polyzwitterionic Brushes. *Science* **2009,** *323* (5922), 1698-1701.
40. Chang, Y.; Shih, Y. J.; Lai, C. J.; Kung, H. H.; Jiang, S. Y., Blood-Inert Surfaces via Ion-Pair Anchoring of Zwitterionic Copolymer Brushes in Human Whole Blood. *Adv. Funct. Mater.* **2013,** *23* (9), 1100-1110.
41. Zhang, Z.; Chao, T.; Chen, S. F.; Jiang, S. Y., Superlow Fouling Sulfobetaine and Carboxybetaine Polymers on Glass Slides. *Langmuir* **2006,** *22* (24), 10072-10077.
42. Kobayashi, M.; Terayama, Y.; Kikuchi, M.; Takahara, A., Chain Dimensions and Surface Characterization of Superhydrophilic Polymer Brushes with Zwitterion Side Groups. *Soft Matter* **2013,** *9* (21), 5138-5148.
43. Kobayashi, M.; Terayama, Y.; Yamaguchi, H.; Terada, M.; Murakami, D.; Ishihara, K.; Takahara, A., Wettability and Antifouling Behavior on the Surfaces of Superhydrophilic Polymer Brushes. *Langmuir* **2012,** *28* (18), 7212-7222.
44. Yu, Y.; Vancso, G. J.; de Beer, S., Substantially Enhanced Stability Against Degrafting of Zwitterionic PMPC Brushes by Utilizing PGMA-Linked Initiators. *Eur. Polym. J.* **2017,** *89*, 221-229.
45. Konkolewicz, D.; Wang, Y.; Krys, P.; Zhong, M.; Isse, A. A.; Gennaro, A.; Matyjaszewski, K., SARA ATRP or SET-LRP. End of Controversy? *Polym. Chem.* **2014,** *5* (15), 4396-4417.
46. Konkolewicz, D.; Krys, P.; Góis, J. R.; Mendonça, P. V.; Zhong, M.; Wang, Y.; Gennaro, A.; Isse, A. A.; Fantin, M.; Matyjaszewski, K., Aqueous RDRP in the Presence of Cu^0: The Exceptional Activity of Cu^I Confirms the SARA ATRP Mechanism. *Macromolecules* **2014,** *47* (2), 560-570.

47. Konkolewicz, D.; Wang, Y.; Zhong, M.; Krys, P.; Isse, A. A.; Gennaro, A.; Matyjaszewski, K., Reversible-Deactivation Radical Polymerization in the Presence of Metallic Copper. A Critical Assessment of the SARA ATRP and SET-LRP Mechanisms. *Macromolecules* **2013,** *46* (22), 8749-8772.
48. Jordan, R.; Ulman, A.; Kang, J. F.; Rafailovich, M. H.; Sokolov, J., Surface-Initiated Anionic Polymerization of Styrene by Means of Self-Assembled Monolayers. *J. Am. Chem. Soc.* **1999,** *121* (5), 1016-1022.
49. Singh, N.; Cui, X. F.; Boland, T.; Husson, S. M., The Role of Independently Variable Grafting Density and Layer Thickness of Polymer Nanolayers on Peptide Adsorption and Cell Adhesion. *Biomaterials* **2007,** *28* (5), 763-771.
50. Ramakrishna, S. N.; Cirelli, M.; Kooij, E. S.; Klein Gunnewiek, M.; Benetti, E. M., Amplified Responsiveness of Multilayered Polymer Grafts: Synergy between Brushes and Hydrogels. *Macromolecules* **2015,** *48*, 7106-7116.
51. Cheng, N.; Brown, A. A.; Azzaroni, O.; Huck, W. T. S., Thickness-Dependent Properties of Polyzwitterionic Brushes. *Macromolecules* **2008,** *41* (17), 6317-6321.
52. Busuttil, K.; Geoghegan, M.; Hunter, C. A.; Leggett, G. J., Contact Mechanics of Nanometer-Scale Molecular Contacts: Correlation between Adhesion, Friction, and Hydrogen Bond Thermodynamics. *J. Am. Chem. Soc.* **2011,** *133* (22), 8625-8632.
53. Hurley, C. R.; Leggett, G. J., Influence of the Solvent Environment on the Contact Mechanics of Tip-Sample Interactions in Friction Force Microscopy of Poly(ethylene terephthalate) Films. *Langmuir* **2006,** *22* (9), 4179-4183.
54. Jiang, S. Y.; Cao, Z. Q., Ultralow-Fouling, Functionalizable, and Hydrolyzable Zwitterionic Materials and Their Derivatives for Biological Applications. *Adv. Mater.* **2010,** *22* (9), 920-932.
55. Shivapooja, P.; Yu, Q.; Orihuela, B.; Mays, R.; Rittschof, D.; Genzer, J.; Lopez, G. P., Modification of Silicone Elastomer Surfaces with Zwitterionic Polymers: Short-Term Fouling Resistance and Triggered Biofouling Release. *ACS Appl. Mater. Interfaces* **2015,** *7* (46), 25586-25591.
56. Sauerbrey, G. Verwendung von Schwingquarzen zur Wägung dünner Schichten und zur Mikrowägung. *Z. Phys.* **1959**, *155*, 206-222.
57. Hilfiker, J. N.; Synowicki, R. A.; Bungay, C. L.; Carpio, R., Spectroscopic Ellipsometry for Polymer Thin Films. *Solid State Tech.* **1998,** *41* (10), 101.
58. Hutter, J. L.; Bechhoefer, J., Calibration of Atomic-Force Microscope Tips. *Rev. Sci. Instrum.* **1993,** *64* (7), 1868-1873.
59. Green, C. P.; Lioe, H.; Cleveland, J. P.; Proksch, R.; Mulvaney, P.; Sader, J. E., Normal and Torsional Spring Constants of Atomic Force Microscope Cantilevers. *Rev. Sci. Instrum.* **2004,** *75* (6), 1988-1996.
60. Cannara, R. J.; Eglin, M.; Carpick, R. W., Lateral Force Calibration in Atomic Force Microscopy: A New Lateral Force Calibration Method and General Guidelines for Optimization. *Rev. Sci. Instrum.* **2006,** *77* (5).
61. Carlmark, A.; Malmstrom, E. E., ATRP Grafting from Cellulose Fibers to Create Block-Copolymer Grafts. *Biomacromolecules* **2003,** *4* (6), 1740-1745.

Table of Contents

Growing Polymer Brushes from a Variety of Substrates under Ambient Conditions by Cu^0-Mediated Surface-Initiated ATRP

Wenqing Yan, Marco Fantin, Shivaprakash Ramakrishna, Nicholas D. Spencer, Krzysztof Matyjaszewski, Edmondo M. Benetti